

BER estimation of QPSK homodyne detection with carrier phase estimation using digital signal processing

Gilad Goldfarb and Guifang Li

College of Optics & Photonics/CREOL&FPCE, University of Central Florida
4000 Central Florida Blvd., Orlando, FL 32816-2700
gilad@creol.ucf.edu, li@creol.ucf.edu

Abstract: An approximate analytical expression for the bit error rate of a QPSK homodyne receiver employing digital signal processing for carrier recovery is derived. BER estimated using the analytical expression is in excellent agreement with Monte-Carlo simulations. The analytical approximation leads to an intuitive understanding of the trade off in such systems and allows optimization of system parameters without resorting to Monte-Carlo simulations.

©2006 Optical Society of America

OCIS codes: (060.1660) Coherent communications; (060.2920) Homodyning

References and Links

1. L. Kazovsky, S. Benedetto, and A. Willner, *Optical Fiber Communication Systems* (Artech House Inc., 1996).
2. R. Noe, "PLL-free synchronous QPSK polarization multiplex/diversity receiver concept with digital I & Q baseband processing," *IEEE Photon. Technol. Lett.* **17**, 887-889 (2005).
3. D. Ly-Gagnon, S. Tsukamoto, K. Katoh, and K. Kikuchi, "Coherent detection of Optical Quadrature Phase-shift keying signals with carrier phase estimation," *J. Lightwave Technol.* **24**, 12-21 (2006).
4. M. G. Taylor, "Coherent detection method using DSP for demodulation of signal and subsequent equalization of propagation impairments," *IEEE Photon. Technol. Lett.* **16**, 674-676 (2004).
5. W. C. Lindsey, and M. K. Simon, *Telecommunication Systems Engineering* (Prentice-Hall Inc., 1973).
6. M. K. Simon, "On the Bit-Error probability of differentially encoded QPSK and offset QPSK in the presence of carrier synchronization," *IEEE Transactions on Comm.* **54**, 806-812 (2006).
7. J. Salz, "Modulation and detection for Coherent Lightwave Communications," *IEEE Comm. Mag.* **24**, 38-49 (1986).
8. G. Casella, and R. L. Berger, *Statistical Inference*, 2nd Ed. (Pacific Grove, CA: Thomson Learning, 2002).

1. Introduction

Coherent detection (CD) is continuously being studied because of its potential advantages over direct detection (DD) [1]. CD generally results in higher sensitivity in optical communication links. CD also results in better channel selectivity in wavelength-division multiplexed optical networks. In CD, the best sensitivity is achieved when homodyne detection is used. However, in this case both the transmitter and local oscillator (LO) lasers need to have narrow linewidths (LWs) and be phase-locked. These requirements render the realization of a homodyne detection receiver difficult to implement. To circumvent this problem, several receiver schemes employing high-speed digital signal processing (DSP) have been suggested [2-4]. These schemes maintain the advantages of homodyne detection without phase locking, using instead digital feedforward carrier recovery.

The scheme in [3] demonstrates an intuitive approach to feedforward carrier estimation for optical QPSK using DSP. Because of its simple implementation, this scheme can potentially be employed in the near future. However, to the best of our knowledge, an analytical derivation of the bit error rate (BER) for this scheme has not been provided in the literature.

Such derivation is valuable towards understanding the effect that each parameter has on the system performance and enables a comparison between various receiver types without the need to revert to time-consuming Monte-Carlo (MC) simulations.

In this paper, we set to find an estimate of the BER for a QPSK feedforward carrier recovery scheme using DSP. The paper is organized as follows: Section 2 presents in detail the feedforward carrier and data recovery scheme employing DSP. The derivation of the phase estimation error associated with this scheme is provided in Section 3. Section 4 presents comparisons between MC simulations and the approximate analytical expression obtained for the distribution of the phase estimation error and the associated BER. Conclusions are presented in section 5.

2. Feedforward carrier recovery using DSP

We begin by presenting the carrier and data recovery process for a DSP based CD receiver. CD of the incoming optical signal is achieved using a phase diversity receiver followed by a pair of balanced detectors, one for each quadrature [1]. The local oscillator (LO) in this scheme is not phase-locked to the carrier, greatly reducing the complexity of the CD process. Analog to digital conversion (ADC) of the two quadratures is performed at the symbol rate (e.g., 10Gsamples/s/quadrature for a 20Gbps QPSK signal). Each pair of samples (the in-phase and quadrature samples) is combined into a single complex sample. The digital feedforward carrier recovery scheme, as suggested in [3], is shown in Fig. 1. The incoming sample stream is divided into blocks of Nb samples each. Each sample block is used as input to the next available processing unit (PU), until the last PU is reached. At that point the first PU should be available to receive the next sample block. The scheme can be generalized to any number of PUs, noting that this continuous process requires that enough PUs are present to allow each PU the necessary time to complete its operation before a new sample block is fed to it. Each PU also requires input from the next PU which is necessary for correct data decoding and phase tracking, as will be discussed later.

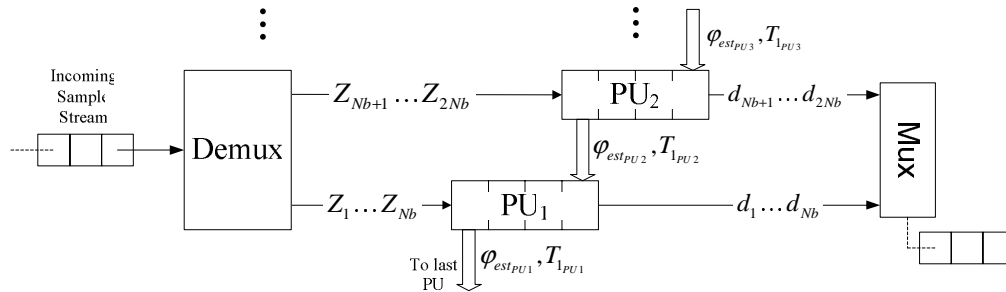


Fig. 1. Schematic of feedforward carrier recovery using DSP

Figure 2 shows the PU block diagram. The operation of each PU is described as follows (details are provided for the first PU, without loss of generality): each complex sample can be written as $Z_k = e^{j(\varphi_{d_k} + \varphi_k)} + n_k$ where $\varphi_{d_k} = (d_k + 1/2) \cdot \pi/2$, φ_k and n_k are the data phase modulation, carrier phase error (with the LO phase as reference) and shot noise, respectively. d_k is the quadrant number of the k^{th} QPSK symbol, taking integer values between 0 and 3. The random process n models the shot noise in the system and is associated with a complex zero mean Gaussian distribution characterized by $n \sim N(0, \sigma_n^2)$. The notation $X \sim N(\mu, \sigma^2)$ signifies that random variable (RV) X is Gaussian distributed with mean μ and variance σ^2 . The only optical impairment incorporated in this model is laser phase noise.

Various other impairments (e.g., amplified spontaneous emission from optical amplifiers, quantization noise inherent in the ADC process and the effect of laser relative intensity noise observed with imperfect balanced detection) are not considered in this work.

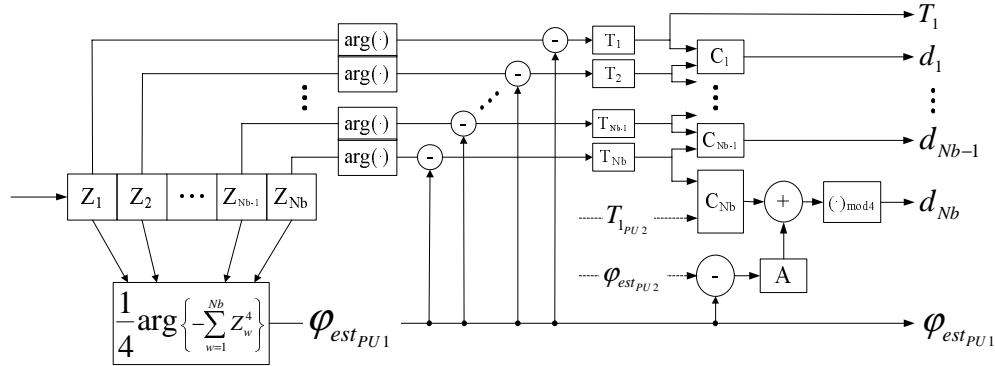


Fig. 2. Processing unit block diagram

In order to obtain the phase estimate for each sample, the QPSK data modulation can be eliminated by calculating Z_k^4 . In the absence of shot noise this operation yields the quantity $-e^{j4\phi_k}$ since $4\phi_k = 2\pi \cdot \text{integer} + \pi$, regardless of d_k 's value. Recalling that ϕ_k is the phase noise term, the operation $1/4 \cdot \arg(-Z_k^4)$ seems to contain complete information about the phase noise at each sample. Unfortunately, there are two sources of error to consider here. The factor of $1/4$ in this operation introduces a 4-fold phase ambiguity which may be eliminated by employing differential precoding of the data quadrant d_k [2, 3, 5]. Another source of error to consider is the ubiquitous shot noise which distorts the phase estimation for each sample. In order to mitigate this effect, an equal-tap weight transversal filter is employed [2]. In this case the carrier phase estimate, $\phi_{est_{PU1}} \in (-\pi/4, \pi/4)$, is common to all the samples in the block and is given by [3]:

$$\phi_{est_{PU1}} = \frac{1}{4} \arg \left\{ -\sum_{w=1}^{Nb} Z_w^4 \right\} \quad (1)$$

It is crucial to note that although the filtering process reduces the effect of shot noise, it will inherently introduce an error on the phase estimation since $\phi_{est_{PU1}}$ is used as a common phase estimate for all the samples in the block. There is an evident tradeoff here: a longer filter (larger Nb) reduces the shot noise more but the phase estimate is then common on more samples, thus reducing the phase estimate accuracy on each sample. Conversely, a shorter filter (ideally $Nb = 1$, i.e., no filtering at all) allows better following of the phase noise in the absence of shot noise, but will perform poorly in the presence of it. An optimal block size can be determined as will be shown later. In order to decode the differentially encoded data, the phase threshold operator T extracts the i^{th} symbol quadrant: $T_i = \lfloor (\arg\{Z_i\} - \phi_{est_{PU1}}) / (\pi/2) \rfloor$, where the $\lfloor X \rfloor$ operator eliminates fractional part of X . Note that this detection scheme is not equivalent to the worse-performing differential detection scheme [5]. Synchronous CD is still employed here where the decoding of the data is performed on the basis of comparison of consecutive quadrant numbers, not pair-wise comparison of sample phases. The operator C

decodes the data such that $d_i = (T_i - T_{i-1})_{\text{mod}4}$; $\forall i = 1..Nb-1$. To decode the last symbol quadrant in PU₁, the first symbol quadrant from PU₂ and its phase estimate (i.e., $T_{1_{PU_2}}, \varphi_{est_{PU_2}}$ when decoding $d_{Nb_{PU_1}}$) are used. $d_{Nb} = (T_{1_{PU_2}} - T_{Nb_{PU_1}} + A(\varphi_{est_{PU_2}} - \varphi_{est_{PU_1}}))_{\text{mod}4}$ where $A(x) = 1$ if $x > \pi/4$, -1 if $x < -\pi/4$ and 0 otherwise. This rather complex operation needed to decode the last symbol in each PU is explained by the fact that the differential encoding employed dictates that only $Nb-1$ decoded symbols can be extracted from Nb samples. To decode the last symbol, the quadrant number of the first sample in the next PU is required.

The BER of a differentially encoded QPSK signal with noisy phase reference can be derived in a similar manner as described in [6, Eq. (12)], although the phase estimation error on two consecutive samples ($\varepsilon_1, \varepsilon_2$) are not assumed to be identical here:

$$\begin{aligned}
 P_e &= \frac{1}{2} \int_{-\pi/4}^{\pi/4} \text{erfc} \left(\sqrt{2\gamma_b} \cdot \cos \left(\frac{\pi}{4} + \varepsilon_1 \right) \right) \cdot P_{\Delta\varphi}(\varepsilon_1) \cdot d\varepsilon_1 \cdot \\
 &\quad \cdot \int_{-\pi/4}^{\pi/4} \text{erfc} \left(-\sqrt{2\gamma_b} \cdot \sin \left(\frac{\pi}{4} + \varepsilon_2 \right) \right) \cdot P_{\Delta\varphi}(\varepsilon_2) \cdot d\varepsilon_2 \quad (2) \\
 &\approx \int_{-\pi/4}^{\pi/4} \text{erfc} \left(\sqrt{\gamma_b} (\cos(\varepsilon) - \sin(\varepsilon)) \right) \cdot P_{\Delta\varphi}(\varepsilon) \cdot d\varepsilon
 \end{aligned}$$

where $\gamma_b = E_b/N_0$ is the electrical signal to noise ratio (SNR) per bit, E_b is the energy per bit and N_0 is the single-sided power spectral density of the shot noise. $P_{\Delta\varphi}\{\varepsilon\}$ is the probability density function (PDF) of the RV $\Delta\varphi$, the phase estimation error.

Note that the simplification taken in Eq. (2) is made under the assumption that $\gamma_b \gg 1$ and a small phase estimation error. These conditions are easily met in the range of parameters (SNR > 6dB and beat LW < 2MHz) considered in this paper. There is a factor of approximately 2 when Eq. (2) is compared to the BER expression for the gray coded case (i.e., no differential encoding) [6, Eq. (14)]. This factor originates from differential encoding where any error in a symbol is manifested twice through differential decoding, to the first-order approximation. From Eq. (2) it is seen that in order to evaluate P_e it is necessary to obtain $P_{\Delta\varphi}$, the distribution of $\Delta\varphi$.

3. Distribution of the phase estimation error - $\Delta\varphi$

The phase estimation error associated with the scheme presented in Fig. 2 is defined by:

$$\Delta\varphi_k = \varphi_k - \frac{1}{4} \arg \left\{ -\sum_{w=1}^{Nb} Z_w^4 \right\} \quad (3)$$

To see how $\Delta\varphi$ is distributed, start by considering the $(\cdot)^4$ operation:

$$Z_w^4 = \left(e^{j(\varphi_{d_w} + \varphi_w)} + n_w \right)^4 = -e^{j4\varphi_w} + 4 \cdot \rho_w + o(n_w^3) \quad (4a)$$

$$\text{where } \rho_w = n_w \cdot e^{j3(\varphi_{d_w} + \varphi_w)} \left(1 + 1.5 \cdot e^{-j(\varphi_{d_w} + \varphi_w)} n_w \right). \quad (4b)$$

For high SNR, all terms containing the shot noise of third order and higher can be neglected because $o(n^3) \ll n^2$. Subsequent simulation results and analytical considerations will confirm the validity of this assumption for high SNR values. Substituting Eq. (4) into Eq. (3), while making this approximation, yields:

$$\Delta\varphi_k \cong \varphi_k - \frac{1}{4} \arg \left\{ \sum_{w=1}^{Nb} \left[e^{j4\varphi_w} - 4 \cdot \rho_w \right] \right\}. \quad (5)$$

We consider first the phase estimation error in the absence of shot noise. Recall that although shot noise is not considered at first, the filtering operation necessary for optimal phase tracking in the presence of shot noise introduces an error on the phase estimation. We set to investigate this error before introducing the shot noise. The phase estimation error in this case is given by:

$$\Delta\varphi_k \cong \varphi_k - \frac{1}{4} \arg \left\{ \sum_{w=1}^{Nb} e^{j4\varphi_w} \right\} = \varphi_k - \varphi_1 - \frac{1}{4} \arg \left\{ 1 + e^{j4(\varphi_2 - \varphi_1)} + \dots + e^{j4(\varphi_{Nb} - \varphi_1)} \right\}. \quad (6)$$

Eq. (6) may be simplified by noting that the laser phase noise is a Wiener process [7] characterized by a zero mean white Gaussian frequency noise $\delta \sim N(0, \sigma_\delta^2 = 2\pi \cdot 2\Delta\nu/B_r)$ where $2\Delta\nu$ and B_r are the beat LW of the transmitter and LO laser, and symbol rate, respectively. The frequency noise is independent of data modulation and shot noise. The instantaneous phase φ_k may then be written as $\varphi_k = \sum_{q=1}^k \delta_q$, where δ_q is the carrier frequency noise at time $q = p/B_r$. The phase difference within a time interval of n/B_r is then given by:

$$\varphi_m - \varphi_{m-n} = \sum_{q=1}^m \delta_q - \sum_{q=1}^{m-n} \delta_q = \sum_{q=m-n+1}^m \delta_q \quad (7)$$

Hence,

$$\Delta\varphi_k = \varphi_k - \varphi_1 - \frac{1}{4} \arg \{ B(Nb) \} \quad (8a)$$

where

$$B(Nb) = 1 + \sum_{w=2}^{Nb} \exp \left\{ j \cdot 4 \sum_{p=2}^w \delta_p \right\}. \quad (8b)$$

$B(Nb)$ can be derived through an example for the case of $Nb = 4$. $B(4) = 1 + \exp\{j \cdot 4\delta_2\} (1 + \exp\{j \cdot 4\delta_3\} (1 + \exp\{j \cdot 4\delta_4\}))$. Assuming that $\left| 4 \sum_{p=2}^w \delta_p \right| \ll 1$, $\forall w = 2, 4$, one may use the fact that $1 + j \cdot x \cong e^{j \cdot x}$ for $x \ll 1$ to approximate $B(4) \cong 4 + j \cdot 4(3\delta_2 + 2\delta_3 + \delta_4) \cong 4 \cdot \exp\{j \cdot (3\delta_2 + 2\delta_3 + \delta_4)\}$. In general, the approximated expression for $B(Nb)$ is given by:

$$B(Nb) \equiv Nb \cdot \exp\{j \cdot 4 \cdot \theta(Nb)\} \quad (9a)$$

$$\text{where } \theta(Nb) = \frac{1}{Nb} \sum_{p=0}^{Nb-2} (p+1) \delta_{Nb-p}, \quad (9b)$$

both valid assuming $\left| \frac{4}{Nb-1} \sum_{p=0}^{Nb-2} (p+1) \delta_{Nb-p} \right| \ll 1$, which can be shown to be valid within the range of SNR of interest. Hence, $\Delta\varphi_k = \varphi_k - \varphi_1 - \arg\{B(Nb)\}/4 \equiv \varphi_k - \varphi_1 - \theta(Nb)$. Noting that $\Delta\varphi_k$ is a linear combination of independent identically distributed (iid) Gaussian RVs, which may be written conveniently in a matrix notation:

$$\begin{bmatrix} \Delta\varphi_1 \\ \vdots \\ \Delta\varphi_{Nb} \end{bmatrix} \equiv \frac{1}{Nb} \underbrace{\begin{bmatrix} 1-Nb & 2-Nb & & -2 & -1 \\ 1 & 2-Nb & & & \\ & 2 & \ddots & & \\ \vdots & \vdots & \ddots & -2 & \\ 1 & 2 & & Nb-2 & -1 \\ & & & Nb-2 & Nb-1 \end{bmatrix}}_M \begin{bmatrix} \delta_2 \\ \vdots \\ \delta_{Nb} \end{bmatrix}.$$

The variance of $\Delta\varphi$ is the sum of the variances of the independent, identically-distributed RVs, so that

$$\Delta\varphi \sim N\left(0, \frac{\sigma_\delta^2}{Nb} \cdot \sum_{p=1}^{Nb} \sum_{q=1}^{Nb-1} M_{p,q}^2 = \frac{Nb^2-1}{6 \cdot Nb} \cdot \sigma_\delta^2\right).$$

We proceed to incorporate the shot noise contribution to the distribution of $\Delta\varphi$. Eq. (5) can be re-written as

$$\Delta\varphi_k = \varphi_k - \varphi_1 - \frac{1}{4} \arg\left\{ B(Nb) + 4 \cdot e^{-j4\varphi_1} \cdot \sum_{w=1}^{Nb} \rho_w \right\} \equiv \sum_{q=2}^{Nb} M_{k,q} \cdot \delta_q - \frac{1}{4} \arg\left\{ 1 + \frac{4}{Nb} \sum_{w=1}^{Nb} \rho_w \right\}.$$

Noting that the phase of a complex Gaussian white noise is uniformly distributed as $\arg\{\rho\} \sim U(0, 2\pi)$, any other arbitrarily distributed angle can be lumped into the phase of the shot noise without affecting its statistical attributes. Assuming $\left| \frac{4}{Nb} \sum_{w=1}^{Nb} \rho_w \right| \ll 1$ and noting that $\arg\{1 + |x|e^{j \cdot \arg\{x\}}\} \equiv \text{Im}\{x\}$ for $|x| \ll 1$, this relation may be written as:

$$\Delta\varphi_k \equiv \sum_{q=2}^{Nb} M_{k,q} \cdot \delta_q - \frac{1}{Nb} \sum_{w=1}^{Nb} \text{Im}\{\rho_w\} \quad (10)$$

As the shot noise and phase noise are independent, the shot noise contribution to the variance of $\Delta\varphi$ is additive. To determine this contribution, the distribution of ρ_w is to be established. Let $\rho = n \cdot (1 + 1.5 \cdot n) \cdot e^{j\eta}$ where $\eta \in (0, 2\pi)$ represents an angle with an

arbitrary PDF, independent of the angle of n (note that ρ_w is a random sample of ρ). $E\{n\} = E\{n_x + j \cdot n_y\} = 0$ and $E\{n_x n_y\} = 0$, from independence of shot noise quadratures. $E\{ne^{jn}(1+1.5 \cdot n)\} = E\{e^{jn}\} \cdot E\{n(1+1.5n)\} = 1.5E\{e^{jn}\}E\{n^2\} = 1.5E\{e^{jn}\}E\{n_x^2 - n_y^2 + 2jn_x n_y\} = 0$, since $E\{n_x^2\} = E\{n_y^2\}$. Also, $\text{var}\{ne^{jn}(1+1.5n)\} = 2E\{|n|^3\}E\{\cos(\arg\{n\})\} + E\{|n|^2\} + 1.5^2 E\{|n|^4\}$. $|n|^2$ is a central-chi-square distributed with two degrees of freedom. $\arg\{n\}$ is uniformly distributed: $E\{\cos(\arg\{n\})\} = 0$. From all the above, $\text{var}\{\rho\} = E\{|n|^2\} + 1.5^2 E\{|n|^4\} = \sigma_n^2(1 + 4.5\sigma_n^2)$. Noting that $\text{Im}\{\rho\}$ is one of the quadratures of ρ , its variance is half of that of ρ . Hence, $\text{var}\{\text{Im}\{\rho\}\} = \text{var}\{\rho\}/2 = \sigma_n^2(1 + 4.5\sigma_n^2)/2$.

Even though the term $\text{Im}\{\rho_w\}$ contains a second order shot noise term, which becomes non-Gaussian distributed, the central limit theorem (CLT) may be applied to obtain an approximation of the distribution of $\Delta\varphi$ as a Gaussian [8]:

$$\Delta\varphi \sim \text{N}\left(0, \frac{Nb^2 - 1}{6 \cdot Nb} \cdot \sigma_\delta^2 + \frac{\sigma_n^2(1 + 4.5 \cdot \sigma_n^2)}{2 \cdot Nb}\right). \quad (11)$$

where σ_δ^2 is associated with the beat LW ($\sigma_\delta^2 = 2\pi \cdot 2\Delta\nu/B_r$). For a QPSK signal in the complex baseband representation with normalized symbol power the complex noise variance may be written in terms of SNR (γ_b) as $\sigma_n^2 = 1/(2\gamma_b)$. Eq. (11) may be equivalently represented using either of these parameters. Subsequent plots use γ_b where the proper substitution into Eq. (11) is made when necessary.

Special care should be taken when invoking the CLT, since at high SNR levels the block size Nb which determines the number of summands reduces. Presence of heavy tails might render the CLT approximation invalid beyond first order. However, as the SNR increases, even though Nb becomes smaller, the significance of the 2nd order shot noise is diminished and the distribution of $\Delta\varphi$ approaches Gaussian anyway. To verify the validity of this approach, a series of $5.5 \cdot 10^{11}$ samples following the distribution of RV $\Delta\varphi$ as defined in Eq. (10) was generated using several computers. The beat LW, SNR and block size used were 2MHz and 13.5dB and 8, respectively. The PDF of the obtained series (generated PDF) was compared to a Gaussian PDF defined by Eq. (11), using the same SNR, LW and block size. Figure 3 presents the two PDFs and the associated BERs as these are accumulated under the integral in Eq. (2) as a function of the integration variable. As seen in Fig. 3, the tails of the generated PDF are somewhat wider compared to the Gaussian PDF. However, by observing the respective BER curves, it is seen that this tails' widening does not significantly affect the final BER; i.e. the difference in BER in both cases is negligible (approximately 5%). Note that the series of generated samples must be long enough to allow for enough events at the tails. It is observed on Fig. 3 that the series used is indeed long enough since the BER curve for the generated PDF case levels off at roughly $\Delta\varphi = 0.325$ where the generated PDF still has enough samples to validate this test. Similar results are obtained for a beat LW of 600KHz, SNR of 13dB and Nb of 15 (parameters which also achieve an approximate BER of 10^{-9}). When lower SNR values are considered, the second order noise becomes more significant. However, a higher shot noise level requires tighter filtering, thus Nb is increased. This in turn

improves the accuracy of the Gaussian approximation since the number of summed terms is now increased. The above explanation does not imply that the actual phase estimation error variance is better approximated at a lower SNR, but simply justifies the use of a Gaussian approximation of the phase estimation error PDF at the SNR range under consideration.

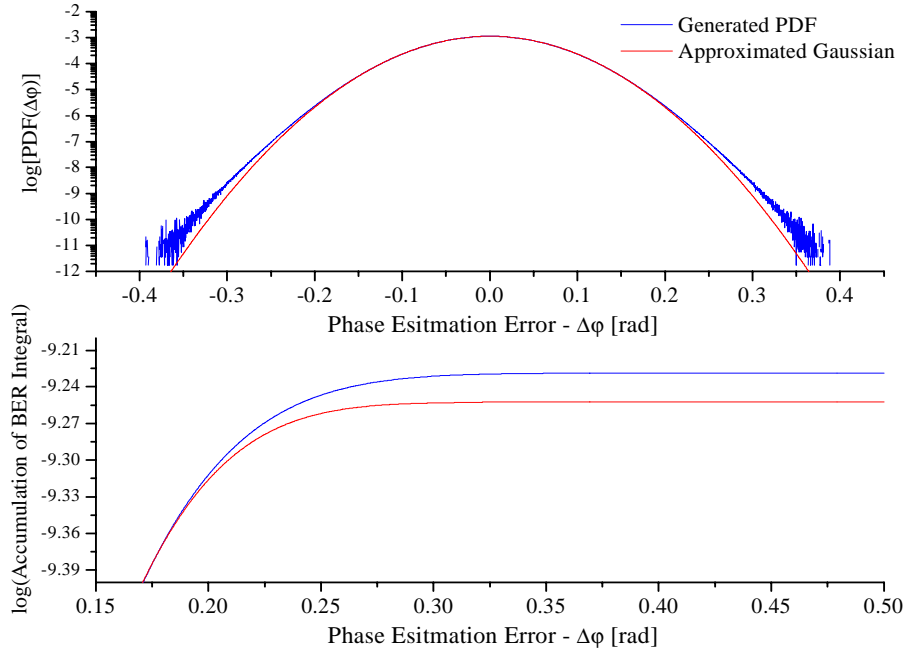


Fig. 3. Top: Generated and approximated PDFs of $\Delta\phi$, Bottom: Accumulation of BER integral for the two PDFs

As can be seen from Eq. (11), the contribution of the phase noise to the variance of $\Delta\phi$ increases with increasing Nb while the impact of shot noise is reduced. Clearly, the expression for the variance of the phase estimation error obtained analytically reflects the tradeoff discussed in section 2. Using Eq. (11), it is possible to find the optimal Nb which gives minimal standard deviation (std) of phase estimation error and hence, smallest BER (considering Eq. 2):

$$Nb_{opt} = \text{round} \left(\sqrt{3 \frac{\sigma_n^2 (1 + 4.5 \cdot \sigma_n^2)}{\sigma_\delta^2} - 1} \right) \quad (12)$$

Figure 4 plots $\log(\text{std}(\Delta\phi))$ as a function of SNR and block size for two beat LWs of 600 KHz [external-cavity distributed-feedback laser (DFB)] and 2 MHz (DFB). The symbol rate used was 10GS/s. Superimposed on these plots is the optimal Nb at each SNR. Note that the log function was used to obtain better contrast on Fig. 4. In this case a lower value is preferable. As seen in Fig. 4, when the SNR is increased, Nb may be reduced as a wider filter becomes sufficient. The result obtained in Eq. (12) is important since it allows an accurate determination of the block size when such a scheme is to be implemented without the need to perform lengthy simulations.

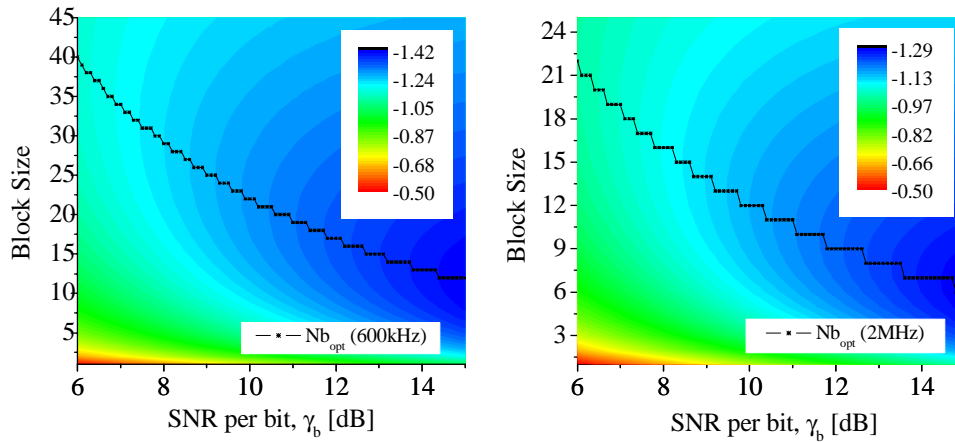


Fig. 4. $\log(\text{std}(\Delta\phi))$ vs. SNR and block size with optimal Nb superimposed. Left: Beat LW of 600kHz, Right: 2MHz.

4. Comparison with Monte-Carlo simulation

MC simulations have been performed to verify the validity of the results obtained in Section 3. A comparison between the MC simulation and approximate analytical expression for $\text{var}(\Delta\phi)$ is presented in Fig. 5. In this case the MC simulations are a strict implementation of the feedforward carrier recovery scheme without any assumptions made on the distribution of the phase estimation error. The MC simulation and analytical approximation show excellent agreement, supporting the approximations made in order to arrive at the analytical expression given in Eq. (11). As expected, the analytical expression is more accurate for smaller LW, which is seen in Fig. 5.

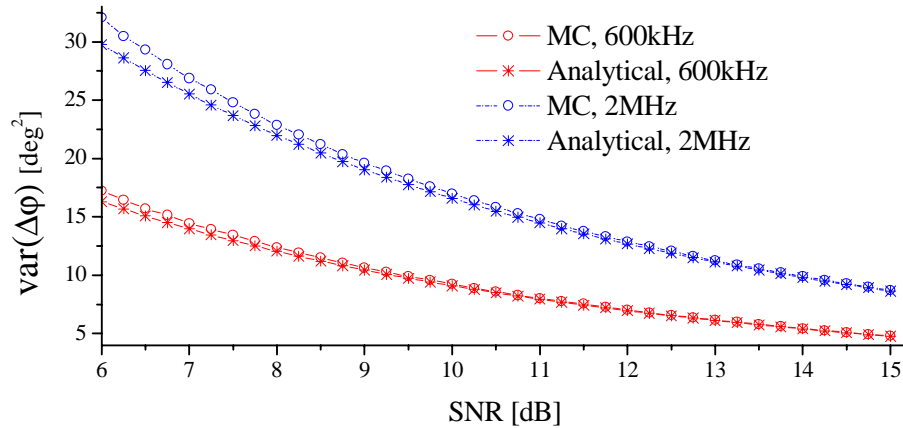


Fig. 5. Comparison of $\text{var}(\Delta\phi)$ from MC simulation and analytical expression

The BER curves obtained from MC simulations were also compared to the approximate BER calculated using Eq. (2) with $\Delta\phi$ distributed as in Eq. (11). The optimal block size for each SNR and LW considered (given in Eq. 12) was used. The BER curves are presented in

Fig. 6. The MC simulations were performed using a series of 10^6 samples. Results of simulations with at least 100 errors are included in the BER comparison. Excellent agreement can be observed between the MC simulation and the obtained analytical approximation. The limit curve shown in Fig. 6 is the numerical evaluation of Eq. (2) taking $P_{\Delta\varphi}(\varepsilon) = \delta(\varepsilon)$. Since the approximations used in the analytical derivation become more accurate with higher SNR, it is expected that the analytical approximation for BER and its MC simulation will have even better agreement at high SNR values.

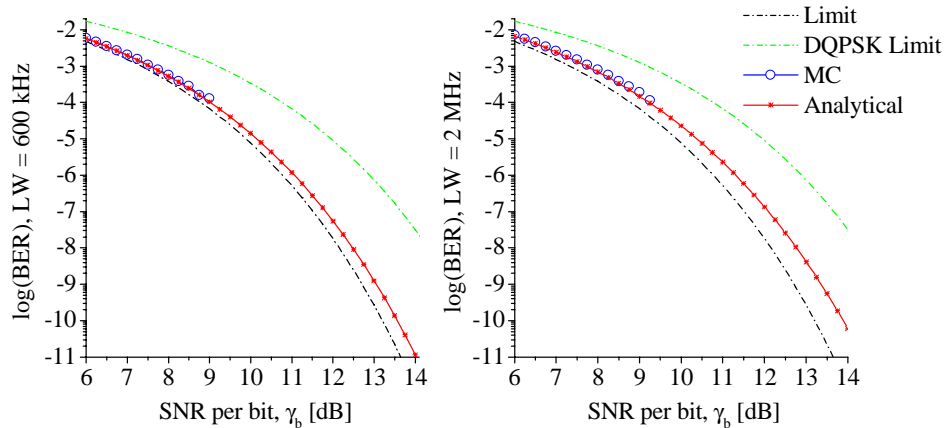


Fig. 6. MC simulation and approximated analytical BER. Left: Beat LW of 600kHz, Right: 2MHz.

As seen in Fig. 6, the use of DSP incurs a small power penalty (e.g., approximately 0.3dB at beat LW of 600kHz for a BER of 10^{-9}) compared to the ideal curve (i.e., no phase estimation error) while avoiding the need to employ carrier phase locking. This simplifies the complexity of a CD receiver dramatically. The DSP based scheme is also observed to significantly outperform the differential QPSK reception. However, it is to be noted that the model considered in the analysis presented does not take into account various other noise sources, as mentioned earlier and may serve as a preliminary, if somewhat optimistic estimation of the DSP based system performance.

5. Conclusion

In this paper, an estimate of the BER for the QPSK feedforward carrier recovery scheme using DSP suggested in [3] was obtained analytically through a series of approximations.

The DSP phase estimation scheme was presented in detail. A 4-fold phase ambiguity associated with this detection scheme was resolved by using differential encoding. It was also determined that shot noise filtering is needed to reduce the effect of shot noise on the phase tracking performance. However, the filtering process itself introduces an error in phase noise tracking. A tradeoff between these two factors is to be addressed where the variable controlling this tradeoff is the PU block size which determines both the width of the shot noise filter and number of samples which share the same phase estimate. Through a series of approximations it was shown that the phase estimation error can be modeled as a zero mean Gaussian RV. The phase estimation error variance was shown to be associated with the beat LW, electrical SNR and block size. Extensive simulation results show that the phase estimation error approximation to Gaussian is viable.

To optimize the system performance (i.e., balance between shot noise filtering and phase noise tracking) the variance of approximated PDF for the phase estimation error was

minimized with respect to the block size, thus obtaining an optimal block size at a given SNR and LW. The values obtained from MC simulations and the analytical expression for the variance of phase estimation error are in excellent agreement.

The analytical approximation allows prediction of the system performance (i.e., BER), for varying parameters. It was observed that the DSP receiver scheme introduces a small power penalty at a BER level of 10^{-9} , compared to the ideal (no phase estimation error) case. The need to phase-lock the LO to the carrier's phase is alleviated, dramatically reducing the complexity of CD reception. Using results obtained in this paper, an intuitive understanding of the design tradeoffs is obtained and optimization may be carried out without reverting to time- and resource- consuming Monte-Carlo simulations.